Experimental Characterization of Woven Jute-Fabric-Reinforced Isothalic Polyester Composites

K. Sabeel Ahmed,[1] S. Vijayarangan[2]

[1]*Department of Production Engineering, PSG College of Technology, Coimbatore 641 004, India*
[2]*Department of Mechanical Engineering, Dr. Mahalingam College of Engineering and Technology, Pollachi 642 003, India*

Received 3 July 2006; accepted 9 October 2006
DOI 10.1002/app.25652
Published online in Wiley InterScience (www.interscience.wiley.com).

ABSTRACT: In this article, mechanical performance of isothalic polyester-based untreated woven jute-fabric composites subjected to various types of loading has been experimentally investigated. The laminates were prepared by hand lay-up technique in a mold. Specimens for tests were fabricated as per ASTM standards. All the tests (except impact) were conducted on closed loop servo hydraulic MTS 810 material test system using data acquisition software Test Works-II. From the results obtained, it was found that the tensile strength and tensile modulus of jute-fabric composite are 83.96% and 118.97% greater than the tensile strength and modulus of unreinforced resin, respectively. The results of other properties, such as flexural, in-plane shear, interlaminar shear, impact, etc., also revealed that the isothalic-polyester-based jute-fabric composite have good mechanical properties and can be a potential material for use in medium load-bearing applications. The failure mechanism and fiber-matrix adhesion were analyzed by scanning electron microscope. Effects of long-term immersion in water on mechanical properties are also presented. © 2007 Wiley Periodicals, Inc. J Appl Polym Sci 104: 2650–2662, 2007

Key words: composites; mechanical properties; fibers; polyester; hand lay up

INTRODUCTION

Conventional fibers, such as kevlar, carbon, aramid, etc., no doubt, gives strong reinforcement in polymer composites but at a very high cost for common and day-to-day applications. Use of such fibers can be justified for aerospace and military applications, where the high cost of the fibers is not of high importance. Hence, there is a growing interest in the use of natural fibers as reinforcement in polymer matrix composites in the recent years. Further, natural fibers offer various advantages over synthetic fiber such as glass, nylon, mica, etc. These advantages[1–3] are low density, low cost, biodegradability, acceptable specific properties, less wear during processing, low energy consumption, etc. Among the natural fibers, jute fiber constitutes the major area of investigation because of its highest content of cellulose when compared with other natural fibers. Also, jute fiber has good thermal and electrical insulation characteristics, appreciable toughness, and as a very important topic, wide commercial availability in various forms at a very low cost. Numerous studies have been carried out by the researchers on natural fiber composites. Moisture absorption characteristics of jute-fiber composites based on polyester and epoxy resin systems, under constant humidity (ø) and ambient temperature (T) conditions have been investigated.[4] It is found that the composite diffusivity is increased with increased fiber volume fraction, whereas the time needed to reach the equilibrium moisture absorption value showed a reversed trend. This behavior is opposite to that observed in the case of composites with impermeable fibers, such as glass, graphite, etc., in the same resin matrices. The mechanical properties of unidirectional jute and glass fibers singly and in combination as a hybrid reinforced in polyester and epoxy resins have been evaluated by authors.[5] Their results showed that the jute-reinforced polyester laminates have much better properties than the resins alone; but the properties are inferior to those of glass-reinforced plastics. The effect of mercerization and silane treatment on mechanical and physical properties of sisal–epoxy composites with different fiber volume fractions has been studied.[6] The authors concluded that mercerization of sisal fibers leads to improved wettability and reduction in water absorption of the sisal–epoxy composites. Mercerization and silane treatment improve the compressive strength without significant effect on flexural properties of sisal epoxy composites. Bamboo fiber/unsaturated polyester,

Correspondence to: K. S. Ahmed (sabil_k@yahoo.com).

Journal of Applied Polymer Science, Vol. 104, 2650–2662 (2007)

$BFRP_{usp}$, (0.68 fiber volume fraction) and bamboo fiber/epoxy, $BFRP_{epoxy}$, (0.63 fiber volume fraction) composites have been developed and their tensile and flexural properties were evaluated and compared.[7] It is found that $BFRP_{usp}$ composites have marginally lower properties than $BFRP_{epoxy}$ composites. It is concluded that the developed material can be used for common commercial applications such as crash helmets, low cost housing, wind-mill fin, etc. A suggestion has been made that the poor interfacial bonding because of the hygroscopic nature of the bamboo fiber can be overcome by using suitable coupling agent. The influence of water uptake on the mechanical properties of jute-fiber-reinforced polypropylene composites has been evaluated by the authors.[8] Jute fibers being hydrophilic absorb a high amount of water causing swelling of fibers. They suggested that swelling of jute fibers in a composite material can have positive effects on mechanical properties. Short pineapple-leaf-fiber-(PALF)-reinforced low-density polyethylene (LDPE) composites were prepared under optimum conditions.[9] The influence of fiber length, fiber loading, and orientation on the mechanical properties has been evaluated. The mechanical properties were found to be enhanced and elongation at break reduced with increasing fiber loading. Longitudinally, oriented composites showed better properties than randomly and transversely oriented composites. They concluded that a comparison of the properties of the PALF-reinforced LDPE composites with those of other cellulose-fiber-reinforced LDPE systems indicated superior performance of the PALF–LDPE composites. The effects of different fiber treatments such as alkali, isocyanate, permanganate, and peroxide on tensile properties of sisal fiber-reinforced LDPE composites were investigated.[10] Alkali-treated fiber showed better tensile properties than untreated composites because of their rough surface topography and increase in aspect ratio. Jochen and Bledzki[11] treated jute fibers with different solutions of NaoH at concentrations up to 28% for a maximum of 30 min at a temperature of 20°C followed by washing of the fibers in distilled water, neutralization with 2 wt % sulfuric acid, washing again, and drying. They found that, at alkali treatment under isometric condition (20 min at 20°C in 25% NaoH solution), the shrinkage of the fiber is 0%, and lead to an increase in the yarn tensile strength and modulus of about 120 and 150%, respectively. The tensile and flexural properties of unidirectional jute/epoxy composites with alkali-treated jute fibers under isometric condition are considerably improved (up to 60% with 0.40 fiber volume fraction). The Young's modulus of untreated jute/epoxy composites is 50% lower than glass fiber/epoxy composites, whereas for alkali-treated jute fiber/epoxy composites, it is 30% lower. Mechanical properties of untreated woven jute fabric reinforced in general purpose polyester resin have been evaluated.[12] The laminates were fabricated with different number of plies for different tests using hand lay-up technique. They concluded that jute/polyester composites have better strength and can be a good substitute for wood. Mohanty et al.[13] investigated the effect of surface modification of two varieties of jute fabrics, i.e., Hessian cloth (HC) and carpet backing cloth (CBC) on tensile, bending, and impact strength of biodegradable jute fabric/biopol composites. Surface modifications like dewaxing, alkali treatment, and cyanoethylation have been carried out. The results indicated that alkali-treated jute-fabric composite has the highest tensile, bending, and impact properties compared to properties of composites treated with other processes. The durability issues of jute-fiber-reinforced phenolic composites have been addressed by evaluating the performance of the composites under various humidity, hygrothermal aging, and weathering conditions.[14] Composites based on phenolic resin with both untreated and alkali and ionized air-treated jute fibers were prepared with different fiber lengths and fiber content.[15] The mechanical properties and morphological aspects of the composites were evaluated by tensile and impact strength and photomicrographs obtained from SEM. Jute-fiber treatment with a solution of 5% NaOH presented the higher tensile strength. The composite reinforced with 5% NaOH-treated fiber showed the highest impact strength when it was combined with ionized air (30% of fiber).

The literature reveals that, though significant amount of work has been carried out on natural fiber composites, none deals with the use of woven jute fabric as reinforcement in isothalic polyester. Also, no single group of researchers has completely characterized the natural fiber composites. In this work, behavior of woven jute-fabric-reinforced isothalic polyester composite under tension, compression, flexural, in-plane shear, interlaminar shear, and impact loading have been experimentally investigated. Elastic properties under tension are predicted by using rule of mixture and compared with measured values. The results of fractographic study and aging effects on mechanical properties are also presented.

EXPERIMENTAL

Materials

Unbalanced plain weave jute fabric 22 × 12 (22 yarns of Tex 310 in warp direction and 12 yarns of Tex 280 in weft direction per inch), having an average weight of 367 g/m^2 and average thickness of

TABLE I
Test Standards and Specimen Dimensions

Property tested	ASTM standard	Rate of loading (mm/min)	Overall length (mm)	Width (mm)	Thickness (mm)	Gauge length/ span (mm)
Tension	3039	2	250	25	6.8	25
Compression	3410	1.5	125	25	6.8	12.7
In-plane shear	3518	2	250	25	6.8	25
Flexural	790	2.8	125	10	6.8	105
ILSS	2344	1.3	45	6.4	6.8	32
Impact	256	–	63	10	10	–

0.8 mm is obtained from Kolkota, West Bengal, India. The resin system consists of isothalic polyester NRC-200-220 supplied by Naphtha Resins and Chemicals, Bangalore, India, cobalt naphthenate accelerator and MEKP catalyst in the ratio of 1:0.015:0.015, respectively.

Laminate fabrication

Laminates of woven jute fabric were prepared by simple hand lay-up technique in a mold at laboratory temperature. PVA-release agent was applied to the surfaces of the mold. Jute-fabric layers were preimpregnated with the matrix material consisting of isothalic polyester, accelerator, and catalyst in the aforementioned ratio. The impregnated layers were placed one over the other in the mold and pressed for 1 h before removal. Provision was made in the mold to allow the hot gases to escape. Uniform thickness was achieved by using spacers of desired thickness between the mold plates. After 1 h, the laminate was removed from the mold and cured at room temperature for 48 h. All the laminates were made with 10 plies with a fiber weight fraction of 43.8% (16 plies for impact test with 47% fiber weight fraction). The fiber volume fraction is calculated using eq. (1) and is found to be 36% (40.8% for impact laminates).

$$V_f = \frac{W_j/\rho_j}{(W_j/\rho_j) + (W_r/\rho_r)} \quad (1)$$

where W_j and W_r are the known weights of the jute and resin, respectively, and ρ_j and ρ_r are the densities of jute and resin, respectively. The density of isothalic polyester is 1.1 g/cm^3, which was obtained from the manufacturer's test report. The jute density, determined from the density of the composite following water-displacement method was found to be 1.42 g/cm^3, which is consistent with the literature.[16]

Specimen fabrication and composite testing

All the specimens were prepared as per ASTM standards. The specimens were carefully cut from the panels using diamond saw with sufficient allowance for finishing. Final dimensions were arrived by finishing the samples using medium grade emery paper. The details of test standards and specimen dimensions are presented in Table I.

All the tests on composite specimens (except impact) were carried out at room temperature on closed loop servo hydraulic MTS 810 Material Test System, having a maximum capacity of 100 kN. Load cell, linear variable differential transformer (LVDT), and extensometer were used to measure force, displacement, and strain, respectively. Data acquisition software Test Works-II was used for testing. The output signal from MTS 458.20 Microconsole controller was converted into digital signal by employing three-channel ADC card. Data were analyzed using MATLAB. Charpy impact test was conducted on instrumented pendulum-type Tinius Olsen Dynatup model 1730 impact tester. In all the cases, five identical specimens were tested and average results were obtained.

Tension test

Tension test was carried out in both warp and weft directions as per ASTM D3039. Aluminum end tabs of 38 mm were bonded on the specimens for proper gripping and to ensure failure in the gauge section. The specimens were loaded in tension at a constant stroke rate of 2 mm/min. Clip-on-type MTS extensometer of gauge length 25 mm was mounted on the specimen for measurement of the strain. For determining the Poisson's ratio, specimens were mounted with strain gauges in longitudinal and lateral directions and the strain was measured using strain indicator B and K type 1526. About 50 kN load cell was used for this test. One group of unreinforced polyester samples was also tested for comparison purpose.

Compression test

Compressive properties such as compressive strength and compressive modulus were determined by static compression test in accordance with ASTM D 3410. The test coupons were cut from the laminates with sufficient allowance in such a way that

jute-warp yarns are oriented in the loading direction. The coupons are then finished to final dimensions using emery paper. Aluminum end tabs of $\sim$ 56 mm length were bonded to the specimens at both the ends to leave a small gauge length of 12.7 mm to avoid buckling of the specimen. Load cell of 20 kN was selected for this test. The load was applied at a constant stroke rate of 1.5 mm/min.

In-plane shear test

In-plane shear properties such as ultimate shear strength and shear modulus were determined by $\pm$ 45° shear test as per ASTM D3518. In this method, uniaxial-tensile loading was applied to the specimen, having the fibers (warp) oriented at $\pm$ 45°. A plot of the shear stress τ_{12} versus shear strain γ_{12} was obtained using the equations, $\tau_{12} = P_x/2A$, and $\gamma_{12} = \epsilon_{xi} - \epsilon_{yi}$, where P_x, A, ϵ_{xi}, and ϵ_{yi} are the load (N), area of cross section (mm^2), longitudinal, and transverse strain, respectively. The chord modulus G_{12} was determined from the slope of the linear portion of the shear stress–shear strain plot.

Flexural test

Flexural test was conducted as per ASTM D 790. Specimens of 125-mm length and 10-mm wide (warp yarns oriented along the lengthwise direction) are loaded in three-point bending with a recommended span to depth ratio of 16:1. The test was conducted using a load cell of 10 kN at 2.8 mm/min rate of loading. The flexural stress in a three-point bending test is given by $\sigma_{max} = (3P_{max}\ L)/(bh^2)$, where P_{max} is the maximum load at failure (N), L is the span (mm), b and h is the width, and thickness of the specimen (mm), respectively. The flexural modulus was calculated from the slope of the initial portion of the load-deflection curve. Flexural modulus is given by $E = (mL^3)/(4bh^3)$, where m is the initial slope of the load deflection curve. One group of unreinforced polyester samples was also tested for comparison purpose.

Interlaminar shear strength

Interlaminar shear strength (ILSS) refers to the shear strength parallel to the plane of the lamination. It is measured in a short-beam test in accordance with ASTM D 2344. A flexural specimen of small span-depth (L/D) ratio is tested in three-point bending to produce a horizontal shear failure between the laminae. As the loading cylinder exerts a downward force, the specimen is subjected to normal (bending), and transverse shear stresses. By using a short beam, it is assumed that the beam is short enough to minimize bending stresses resulting in an interlaminar shear failure, by cracking along a horizontal plane between the laminae. The force applied at the time of failure was recorded and the stresses were determined using the equation $S_H = (0.75\ P_B)/(bd)$, where S_H is the ILSS (N/mm^2), P_B is the breaking load (N), b and d are width (mm), and depth (mm) of the specimen, respectively. About 10 kN-capacity load cell was used and the load was applied at the rate of 1.3 mm/min. Recommended span-depth ratio of 5:1 was used.

TABLE II
Jute Fiber and Isothalic Polyester Resin Properties

Property	Jute fiber	Isothalic polyester
Density (gm/cm^3)	1.45	1.1
Young's modulus (GPa)	20	4.375
Poisson's ratio	0.38	0.46
Shear modulus (GPa)	7.24	1.49

Impact test

The square cross-sectional specimens were impacted by 10-mm hemispherical head. The impact velocity was 0.75 m/s for polyester specimens and jute laminates. The impact events such as load-time, energy-time, and load-deflection plots were recorded.

Theoretical modeling of elastic properties

Assuming uniform distribution of resin in the composite, the average fiber volume fraction in each ply is same as total fiber volume fraction. The tensile-elastic properties of unidirectional jute-fiber lamina were predicted from fiber and resin properties (Table II), using simple rule of mixture relationships from the mechanics of materials approach.[17] The elastic properties (Young's modulus in warp and weft direction and major Poisson's ratio) of 0/90° woven jute-fabric composites were calculated analytically using eqs. (2)–(4)[18] from the elastic properties of unidirectional jute ply.

For woven-jute ply,

$$E_{11} = KE_l + (1 - K)E_t \tag{2}$$

$$E_{22} = (1 - K)E_l + KE_t \tag{3}$$

$$\nu_{12} = \frac{\nu_{lt}}{K + (1 - K)\frac{E_l}{E_t}} \tag{4}$$

where,

$$K = \frac{N_1}{N_1 + N_2} = 0.647 \tag{5}$$

where N_1, N_2 are the number of yarns in warp and weft direction, respectively, E_l, E_t are the Young's modulus for unidirectional jute ply in longitudinal

and transverse direction, respectively, v_{lt} is the major Poisson's ratio of unidirectional jute ply. Since all the plies are oriented in the same direction, the elastic properties of the laminate is same as that of woven ply ($E_x = E_{11}$, $E_y = E_{22}$, and $\upsilon_{xy} = v_{12}$). The chord modulus of woven-jute ply (G_{12}) was same as that for unidirectional jute ply (G_{lt})[18] that was determined from rule of mixture. Again, the laminate shear modulus is same as that of woven ply modulus since all the plies are oriented in the same direction ($G_{xy} = G_{12}$).

Water absorption and its effect on mechanical properties

All polymers and composites absorb moisture in humid atmosphere and when immersed in water. Natural fibers absorb more moisture when compared with synthetic fibers. The effect of this moisture absorption is to degrade the properties such as tensile strength, flexural strength, impact strength, etc. Water absorption test was conducted as per ASTM D570. The test specimens were cut from the laminated panels to the size recommended in ASTM D 570 (76.2 × 25.4) mm. Edges of the samples were sealed with polyester resin. Samples in groups of three were dried in an oven for 24 h at 70°C. The weights of the dry samples were recorded. The samples were then immersed in water at room temperature. Samples were periodically taken out of the water, surface water was wiped off with soft cloth or tissue paper, and weighed to the nearest 0.0001 g, and the samples were reimmersed in water immediately. Weight readings of the samples were taken till the samples reached the equilibrium value. The percentage uptake of water was determined using the eq. (6).

$$M(\%) = \frac{(W_w - W_d)}{W_d} \times 100 \tag{6}$$

where W_w and W_d are the weights of the wet and dry sample, respectively.

On the basis of the Fick's law of diffusion, the moisture weight gain, G as a function of time t, can experimentally be measured by weighing the specimen at various times during exposure to a moist environment. If the material is completely dry prior to exposure to moisture, then initial weight percent of moisture M_i is zero. For shorter period of time (e.g., in terms of days in comparison to years of use in real applications), G can be approximated by the eq. (7).[19]

$$G = \frac{M\%}{M_m\%} = \frac{4}{h}\left(\frac{D_z t}{\pi}\right)^{1/2} \quad \frac{D_z t}{h^2} < 0.05 \tag{7}$$

where M is the mass at any time t, M_m is the weight percent of moisture in the material when it reaches the fully saturated condition, D_z is the mass diffusivity in the composite, and h is the thickness of the laminate. Equation (7) indicates that the moisture absorption depends on the square root of time. Moisture intake in composite materials is therefore plotted as a function of the square root of time. Writing the eq. (7) for two different instances of exposure period t_1 and t_2,

$$\frac{M_1}{M_m} = 4\left[\frac{D_z t_1}{\pi h^2}\right]^{1/2} \tag{8}$$

$$\frac{M_2}{M_m} = 4\left[\frac{D_z t_2}{\pi h^2}\right]^{1/2} \tag{9}$$

Subtracting (8) from (9), and rearranging, we get,

$$D_z = \pi\left[\frac{h}{4M_m}\right]^2\left[\frac{M_2 - M_1}{\sqrt{t_2} - \sqrt{t_1}}\right]^2 \tag{10}$$

Equation (10) shows that if the quantities M_m and the linear slope of the moisture absorption curves, i.e., $(M_2 - M_1)/(\sqrt{t_2} - \sqrt{t_1})$ are known, the composite-diffusion coefficient can be easily evaluated.

Since most moisture diffusion experiments include moisture diffusion through six surfaces, the value of D_z in eq. (10) is in error.[20] For true one-dimensional diffusion coefficient D_z, a correction factor for edge effect given by Shen and Springer[21] can be used giving

$$D = D_z\left(1 + \frac{h}{w} + \frac{h}{l}\right)^{-2} \tag{11}$$

where w and l are the laminate width and length, respectively.

Strength degradation studies are essential to know the long-term behavior of the composites, after being exposed to water or humid atmosphere. The tension, flexural, and ILSS tests were conducted in the same way as mentioned earlier on samples that were immersed in water for two different periods on immersion viz., 30 and 65 days, to evaluate the residual strength of the composite. Three identical samples were tested for each period of immersion and average result was obtained.

Fractography

SEM study was carried out to investigate the mode of fracture such as fiber splitting, fiber pull-out, debonding, matrix cracking, and fiber-matrix adhesion. Samples for examination were obtained by cutting sections about 3–4 mm in length from just below the fracture zone. The fractured surfaces of the samples were sputter coated with the thin layer

of gold to minimize the charging problem using JEOL-fine coat ion sputter, JFC-1100.

The fracture surfaces of the selected tensile, flexural, interlaminar shear, and impact tested specimens were examined using JEOL 6360 software-controlled scanning electron microscope. The instrument was operated at 5 kV.

RESULTS AND DISCUSSION

Jute yarn and fabric test

The failure strength of the jute yarns of warp and weft direction was found by conducting tension tests on atleast 20 samples of jute yarns (320-mm long) as per ASTM 5526 using computer-interfaced Textechno statimat-4 yarns and fabric-testing machine at Textile Committee Laboratory, Coimbatore, South India. Tests were conducted at room temperature using 100-N load cell at the loading rate of 30 mm/min. The failure strength of the yarns of warp direction was found to be 40.79 N and for weft yarns, it is 29.42 N. The jute fabric of size (120 × 25) mm was also tested along warp and weft direction according to ASTM 5035 using load cell of 1000 N at the loading rate of 300 mm/min. Along each direction, five samples were tested and average result was obtained. The failure strength of the fabric in warp direction was found to be 669 N and for weft direction it is 241 N.

Composite testing

A summary of the results obtained for unreinforced polyester and jute-fabric-reinforced composite samples is presented in Table III.

Analysis of tension test results

Figures 1 and 2 represents the tensile stress–strain diagram for jute laminates in warp and weft direction, respectively. The initial portion of the curve is linear at low strain rates followed by change in the slope of the curve indicating nonlinear behavior of the material. The start of nonlinearity in the curve is an indication of the initial matrix cracking followed by progressive failure of the fibers. The average tensile strength of jute laminates was found to be 80.19 MPa in warp and 40.50 MPa in weft direction, respectively. The tensile strength of jute laminate in warp direction is 83.96% higher than the tensile strength of unreinforced polyester samples. The strain at maximum tensile stress for composite samples ranged from 1.38% to 1.78% in warp and 1.05–2.01% in weft direction, respectively. Tensile modulii were determined by the slope of the initial portion of stress–strain curves. A significant improvement in the tensile modulus of polyester samples was obtained by jute-fabric reinforcement. The warp direction tensile modulus was 118.97% higher than the modulus of polyester samples. The measured

TABLE III
Properties Evaluated for Resin and Jute Composite

Property	Resin	Jute composite
Density(g/cm^3)	1.1	1.19 (0.01)
Tension test in warp direction		
Tensile strength (MPa)	43.59 (9.26)[a]	80.19 (5.10)
Tensile modulus (GPa)	4.375 (1.71)	9.58 (0.22)
Strain at break	–	1.57 (0.06)
Poisson's ratio	0.46	0.35
Tension test in weft direction		
Tensile strength (MPa)	–	40.50 (4.92)
Tensile modulus (GPa)	–	5.75 (0.30)
Strain at break	–	1.48 (0.39)
Poisson's ratio	–	0.25
Compression test		
Compressive strength (MPa)	–	83.38 (1.34)
Compressive modulus (GPa)	–	1.84 (0.13)
In-plane shear test		
Shear strength (MPa)	–	20.78 (0.15)
Shear modulus (GPa)	–	1.74 (0.04)
Flexural test		
Flexural strength (MPa)	92.38 (5.64)	121.80 (17.60)
Flexural modulus (GPa)	2.47 (0.18)	7.64 (0.35)
Interlaminar shear test (ILSS)		
Interlaminar shear strength (MPa)	–	13.90 (1.54)
Charpy impact test		
Charpy impact strength (kJ/m^2)	4.477 (0.89)	31.87 (1.21)

Numbers in parenthesis are standard deviations.

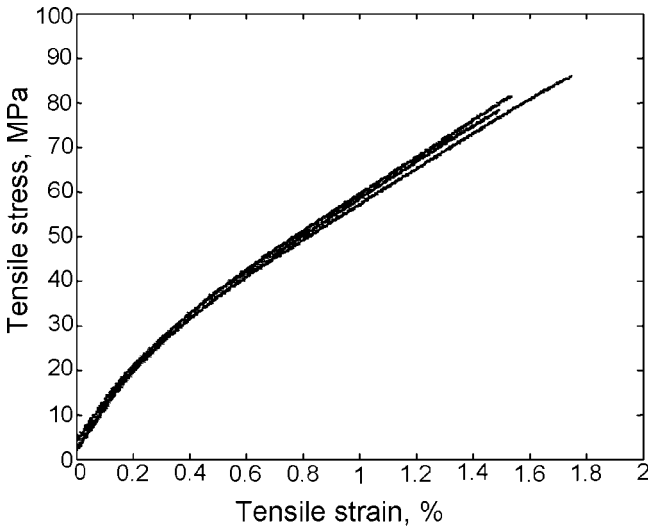

Figure 1 Stress–strain diagram in warp direction.

and predicted values of elastic properties by rule of mixture for woven jute-fabric composite are shown in Table IV. The results depicted in table reveals that predicted values of elastic properties deviate from experimental values by 9 to 15%. This deviation may be because of nonuniformity of jute yarns and poor interfacial bonding between the fiber and matrix. It can be seen from the Table III that tensile properties such as tensile strength, tensile modulus, and Poisson's ratio of jute laminate is higher in warp direction than in weft direction. This is because more number of fibers in warp direction offers greater resistance to crack propagation than in weft direction. As a result, the strength of the material in warp direction is greater than the strength in the weft direction. An observation of failed laminates revealed that the failure is brittle in nature with little

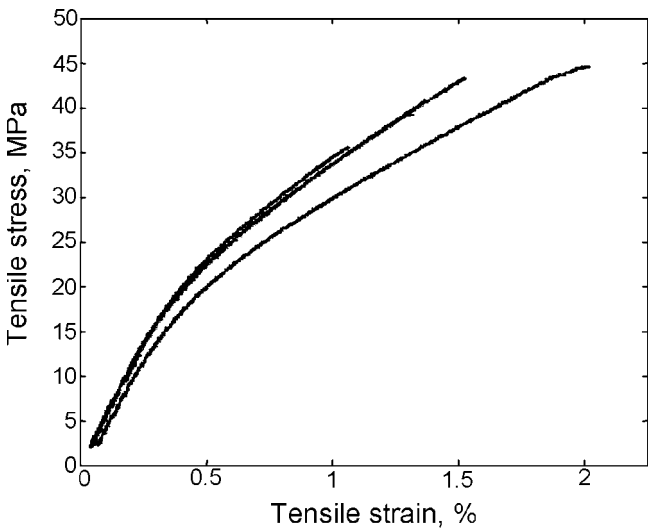

Figure 2 Stress–strain diagram in weft direction.

TABLE IV
Measured and Predicted Values of Elastic Properties

Elastic properties	Measured	Predicted
E_x (GPa)	9.00	8.62
E_y (GPa)	6.50	7.43
ν_{xy}	0.35	0.35
G_{xy} (GPa)	1.90	2.08

or no pull out of jute fibers. This may be because of lesser extensibility of jute fibers (1.5–1.8).[22] In woven fabric, fiber yarns of warp direction crossover and under the fiber yarns of weft direction to create an interlocking structure. Under tensile loading, these crimped fibers tend to straighten out, which create high stresses in the matrix. As a result, a microcrack is initiated in the matrix, which propagates through the fiber-matrix interface, in the transverse direction causing fiber to fracture propagates again into the matrix till the next interface and so on until complete fracture occurs. Figures 3(a,b) shows the SEM image of tensile-fractured surface of jute composite when loaded in warp and weft direction, respectively. Fracture of fiber with little pull out is visible from the image. No evidence or traces of matrix resin adhering to the fiber is an indication of poor fiber-matrix adhesion.

Analysis of compression test results

Figure 4 shows the compressive stress–strain behavior of jute laminates. It can be seen from the figure that the behavior of jute composite under compressive loading is nonlinear. The compressive modulus is obtained from the initial portion of the stress–strain diagram. The experimental results revealed that the average compressive strength of jute laminates is 83.38 MPa, which is almost the same as that of tensile strength of warp direction for the same volume fraction of jute fibers. The compressive modulus is reduced by 80.79% of the tensile modulus in warp direction. The drastic reduction in the compressive modulus is attributed to high percentage strain of the laminates under compressive loading. The strain in the laminates at break under compression test is more than 10%, whereas in tension test, it is just about 1.5. The major failure mechanism noticed in the compression-test samples is fiber microbuckling.

Analysis of in-plane shear test results

The shear stress–shear strain curve for jute laminates was found to be linear only at low shear strain level (Fig. 5). Hence, a lower shear strain range of 2000 με is selected for the determination of chord modulus of elasticity. The point of deviation of the curve from nonlinearity is an indication of beginning of the

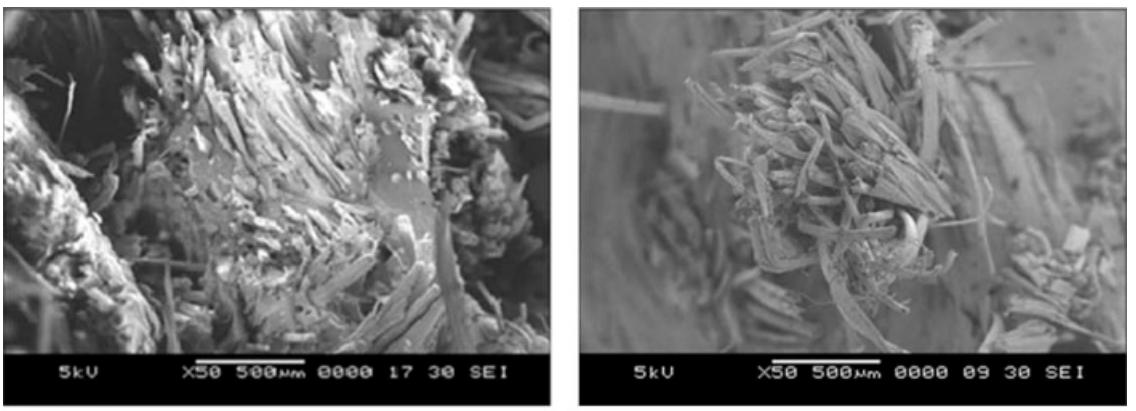

Figure 3 (a) SEM image of tensile-fractured surface (warp direction) and (b) SEM image of tensile-fractured surface (weft direction).

shear failure. All the specimens were failed because of jute-fiber breakage and matrix cracking. The average value of maximum shear stress for jute composite is found to be 20.78 MPa. The shear modulus of jute composite is found to be 1.74 GPa, which is just 16.78% higher than the shear modulus of isothalic polyester (1.49 GPa). The average shear modulus of isothalic polyester was established from the values of Young's modulus (E) and Poisson's ratio (v) of the resin from Table II using the eq. (12).

$$G = \frac{E}{2(1+v)} \tag{12}$$

Analysis of flexural-test results

The load-displacement behavior of jute laminates is presented in Figure 6. Under the flexural loading, the surfaces of the specimen are subjected to greater strains than the sample center. Hence, flexural strength and stiffness is controlled by the strength of the extreme layers of reinforcement.[12] The average flexural strength of jute composite is found to be 121.80 MPa, which is 31.8% higher than the flexural strength of unreinforced polyester resin. The flexural modulus is a measure of the resistance to deformation of the composite in bending. The average flexural modulus of jute composite is found to be 7.64 GPa, which is 209% higher than the modulus of unreinforced resin. The fracture mechanism of the sample can be viewed by SEM images taken normal to tension surface and normal to adjacent surface as shown in Figures 7(a,b), respectively. The failure was seen to occur because of the matrix cracking and fiber breakage at the tension side of the laminates. The failure initiates with the development of crack on the tension side and propagates through

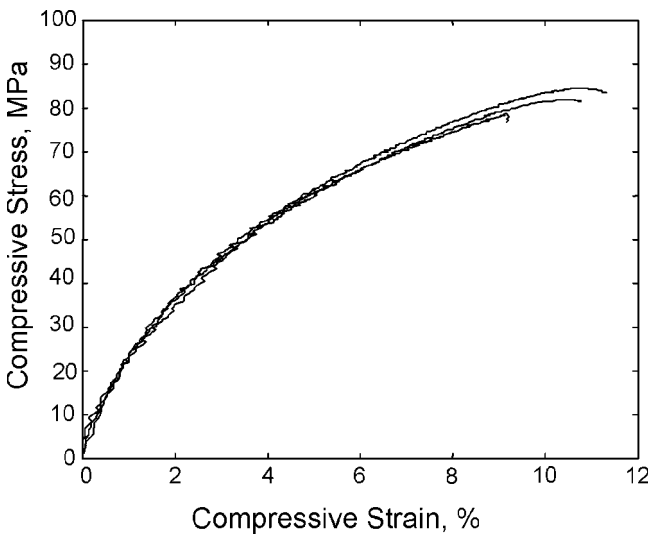

Figure 4 Compressive stress–strain diagram.

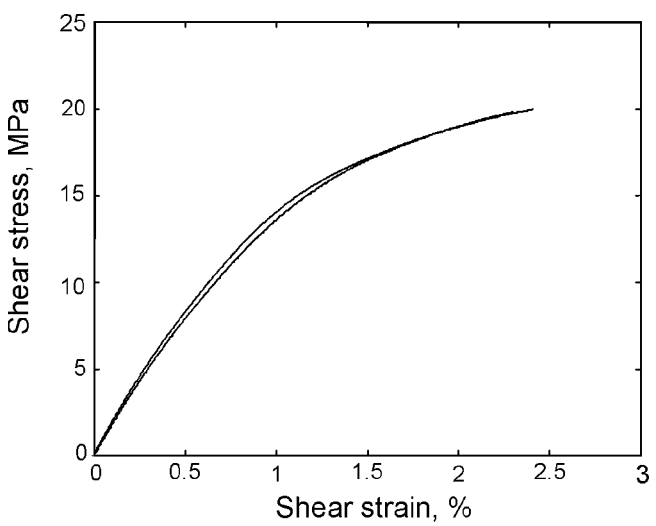

Figure 5 Shear stress–shear strain diagram.

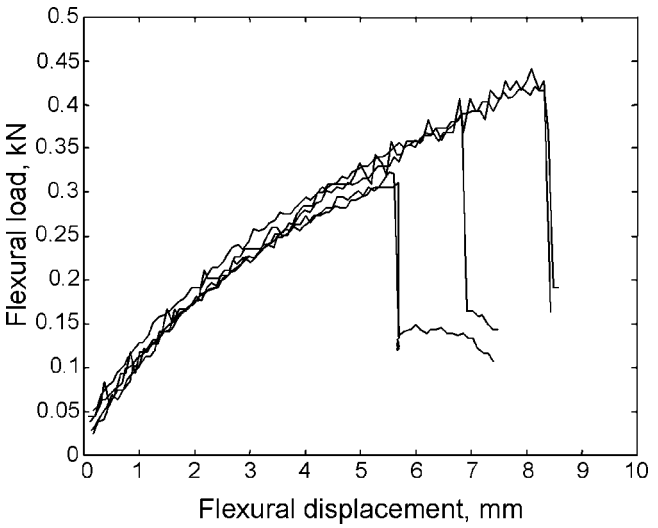

Figure 6 Flexural load-displacement diagram.

the thickness till the failure of the laminate occurs. It was observed that none of the specimens were completely broken at peak load.

Analysis of ILSS test results

The load-displacement plots of interlaminar shear testing are presented in Figure 8. The plots show similar trend as for flexural tests. In short-beam shear tests, the maximum shear stress occurs in an area where other stresses may exist unlike homogeneous beam theory; in which maximum shear stress occurs at the neutral plane where normal stresses were zero. This results in combination of failure modes,[17] such as fiber rupture, microbuckling, and interlaminar shear cracking. Interlaminar shear failure may not also take place at the laminate midplane and it is difficult to ensure pure shear failure along the interface. For these reasons, it is difficult to interpret the short-beam test data. However, jute laminates exhibit an average interlaminar shear stress value of 13.9 MPa. The SEM image of the fractured surface of the specimen under ILSS test shown in Figure 9 indicates that the failure is taken place because of matrix cracking at the tension side similar to failure under flexural loading.

Analysis of impact test results

Figure 10 depicts load and energy curves as a function of time for jute laminates. The incipient load and energy denoted by P_i and E_i in Figure 10 corresponds to the change in the slope in the ascending portion of the load-time or load-deflection curve. At this point, the impact load causes the damage to the matrix material because of internal delamination or fiber-matrix interface failure.[23] However, this damage being negligible has no effect on the strength and stiffness of the composite. The nonlinear portion of the curve beyond the incipient load and energy point indicates the progressive failure of the fibers until the peak load, which is the maximum load that the material can withstand. At peak load, damage because of fiber breakage occurs at the tension side and propagates through the thickness. The load suddenly drops from peak point to the failure point and then to the zero load point with constant slope. The energy corresponding to the peak load is termed as initiation energy, E_m, and propagation energy is given by $E_p = E_t - E_m$, where E_t is the total energy. The propagation energy is a measure of the energy required to propagate the damage (delamination, fiber breakage, matrix cracking, and fiber pullout). The ratio E_p/E_m is termed as ductility index (DI).[24] The average DI for jute laminate is found to be 0.512. Low DI is an indication of brittle nature of the material. The impact strength is determined by

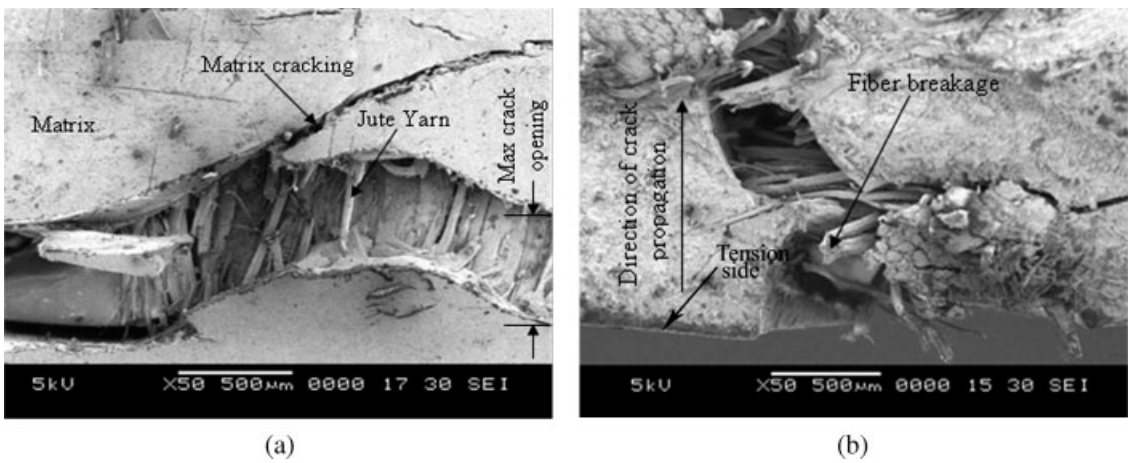

Figure 7 (a) SEM image showing the fracture at the tension surface of flexural sample and (b) SEM image of the fractured adjacent surface showing crack propagation (flexural loading).

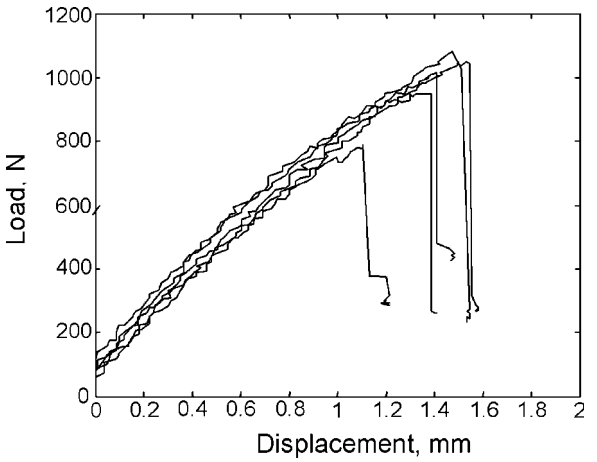

Figure 8 Load-displacement diagram for interlaminar shear test.

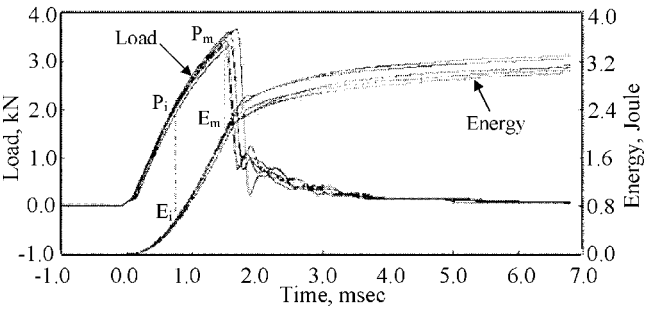

Figure 10 Load-energy-time plot for all jute laminates.

dividing the total energy absorbed by the material with the cross-sectional area. The effect of jute-fiber addition on impact strength of polyester resin is presented in Table III. The average impact strength of jute composite (31.872 kJ/m^2) is 612% higher than the impact strength of unreinforced resin samples. This indicates that the fiber plays an important role in the impact resistance of the composite as they interact with the crack formation in the matrix and act as stress-transferring medium. Observations of the impacted fractured surface of the laminate (Fig. 11) indicate considerable damage of the jute fibers because of splitting from the strands.

Water absorption behavior and its effect on mechanical properties

Figure 12 shows the percentage water absorption in jute composite with respect to square root of time in hours. It can be seen from the figure that the saturation level is reached after 1600 h and maximum water absorbed at saturation level is 13% of the dry sample weight. From the slope of the curve shown in Figure 12, diffusion coefficient was calculated using the eq. (10) and is found to be 7.3487×10^{-7} mm^2/s; however, when the correction factor for edge effect was considered, the diffusion coefficient was reduced to 4.0528×10^{-7} mm^2/s. The mechanical properties of jute composites after immersion in water are found to degrade, which may be because of degradation of its constituents such as fiber and matrix or may be due to weakening of fiber-matrix interface. Degradation in reinforcements plays an important role in strength and stiffness reduction of fiber-reinforced composites as they are the major load-carrying constituents.[25] The high percentage of water absorption (13%) is because of the hydrophilic nature of jute fiber that causes its swelling and shrinkage resulting in weakening of the fiber strength. Water molecules would be attracted by the hydrophilic groups of polyester causing swelling of the matrix. The dimensional instability of the matrix under the influence of water may result in debonding of the fiber/matrix interface. The interfacial adhesion characteristics have a significant effect on the load carrying capacity of a fiber-reinforced composite. When the composites have been immersed in

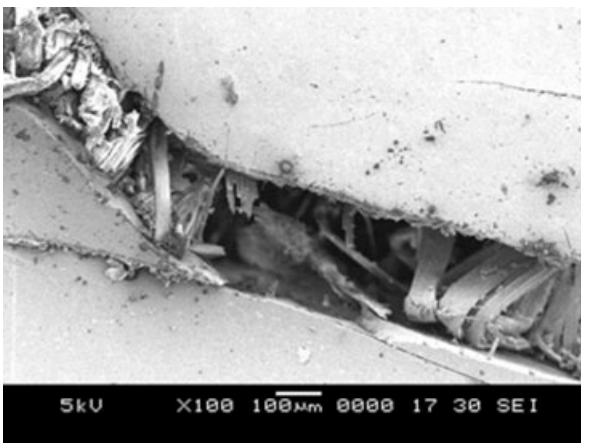

Figure 9 SEM image showing crack in the matrix at the tension surface (ILSS).

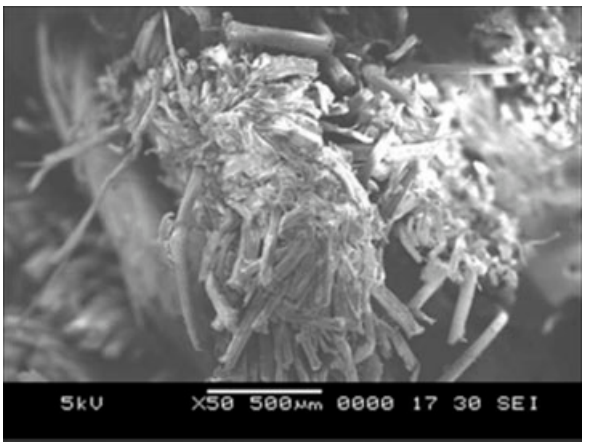

Figure 11 SEM image of impact-fractured surface of jute laminate.

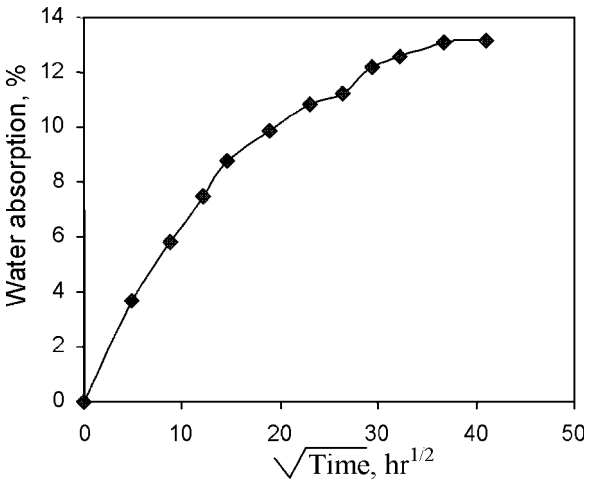

Figure 12 Percentage water absorption V/s square root of time in hours.

water, the capillarity would conduct the water molecules to the material and fills in the voids and cracks in the composites. Such water-filled voids at the interface result in interfacial debonding. Differences in moisture-expansion coefficients of fiber and matrix also contribute to progressive debonding and therefore weakening of the material. Figures 13 and 14 show the variation in tensile properties of jute composite after immersion in water for 30 and 65 days. Jute composite showed negligible reduction (2.4%) in the tensile strength after 30 days of immersion; however, the reduction is significant (12%) for 65 days of immersion in water. The decrease in the tensile modulus of composite for 30 and 65 days of immersion in water is found to be 27.3 and 43%, respectively. The variation in the flexural properties of jute composite for different periods of immersion in water is shown in Figures 15 and 16. Figure 15 reveals that the degradation in flexural strength is significant only in the first period (30 days) with a reduction in the flexural strength of 40%. No further

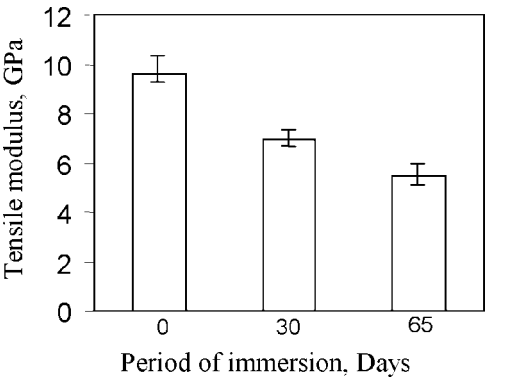

Figure 14 Tensile modulus for different periods of immersion in water.

loss of strength is noticed beyond 30 days of immersion in water. The reduction in flexural modulus of jute composite is 40 and 56% for two different periods of immersion in water, respectively. Figures 17 and 18 show a comparison between fracture mechanism before immersion in water and after 65 days of immersion in water. The damage caused to the fibers as well as loss of matrix resulting in weak fiber-matrix interfacial bonding can be observed from SEM image of fractured surfaces after 65 days of immersion in water. Similar observations can be made for other properties also. The effect of water absorption on ILSS is shown in Figure 18. It appears from the figure that the reduction in ILSS is continuous. A decrease in ILSS of 16.3 and 32% in jute composite was observed, respectively, for the two periods of immersion namely, 30 and 65 days. The main factor that influences the degradation in the properties is weakening of fiber-matrix adhesion as a result of swelling and shrinkage of fibers with the diffusion of water. The moisture absorption of jute composite and hence degradation in the mechanical strength can be substantially reduced by suitable techniques like, surface modification of jute fiber, effective

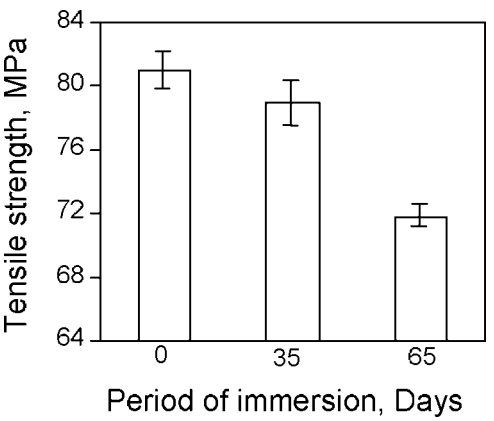

Figure 13 Tensile strength for different periods of immersion in water.

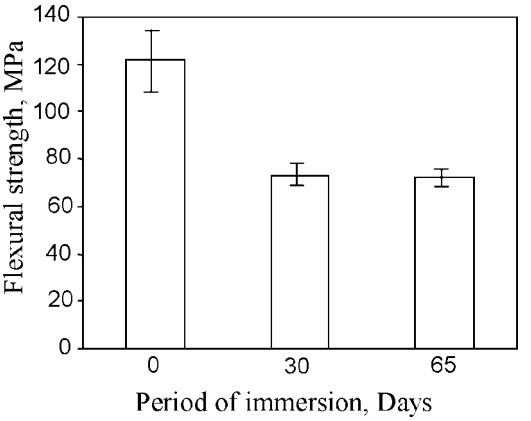

Figure 15 Flexural strength for different periods of immersion in water.

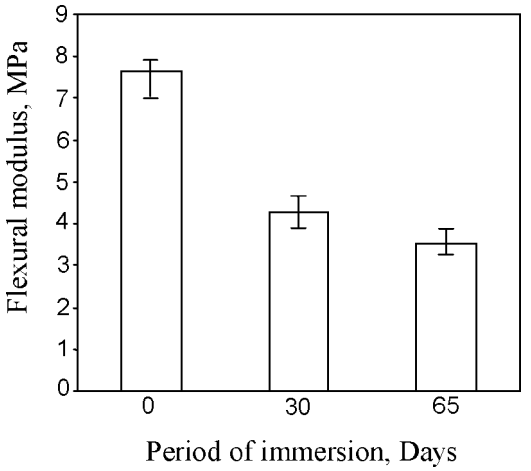

Figure 16 Flexural modulus for different periods of immersion in water.

hybridization with synthetic fiber plies at the extreme to prevent direct contact of jute with water, enamel coating, etc., which is not in the purview of this article.

CONCLUSIONS

The mechanical behavior of isothalic polyester-based untreated woven jute-fabric composite has been investigated under tensile, compressive, in-plane shear, flexural, interlaminar shear, and impact loading using performance curves. Water absorption behavior and its effect on tensile, flexural, and interlaminar shear properties of jute composite are evaluated for different periods of immersion in water. Failure mechanism was studied by SEM images. From this study, the following major conclusions are drawn.

1. The behavior of isothalic polyester-based jute composite under various loading is nonlinear.
2. The tensile strength and tensile modulus of jute-fabric composite are 83.96% and 118.97% greater than the tensile strength and modulus of unreinforced resin, respectively.
3. The average compressive strength of jute composites is almost the same as that of tensile strength in warp direction.
4. The flexural strength and flexural modulus of jute-fabric composite are 31.80 and 209% greater than the flexural strength and flexural modulus of unreinforced resin, respectively.
5. Significant improvement (611%) in the impact strength of resin is obtained by reinforcement with jute fabric with fiber volume fraction of 0.408.
6. Water absorption has detrimental effect on mechanical properties of the composite. Tensile, flexural, and interlaminar shear properties of jute composite are found to degrade on immersion in water for different periods.
7. The degradation in tensile strength is significant after 30 days of immersion in water, whereas degradation in flexural strength is significant within 30 days.
8. The mechanical properties of isothalic polyester-based jute composite are greater than general purpose polyester-based-jute composite,[12] but less than that of glass composite.

Finally, it can be concluded that isothalic polyester-based jute composite can be a good substitute for wood and are suitable for low load bearing applications like partition walls, interior decoration, doors, false ceilings, seat backs, luggage shelves, machine covers, etc.

The authors are thankful to the Director and staff of Structures and Materials Division, Aeronautical Development Establishment, Bangalore, for providing us the testing

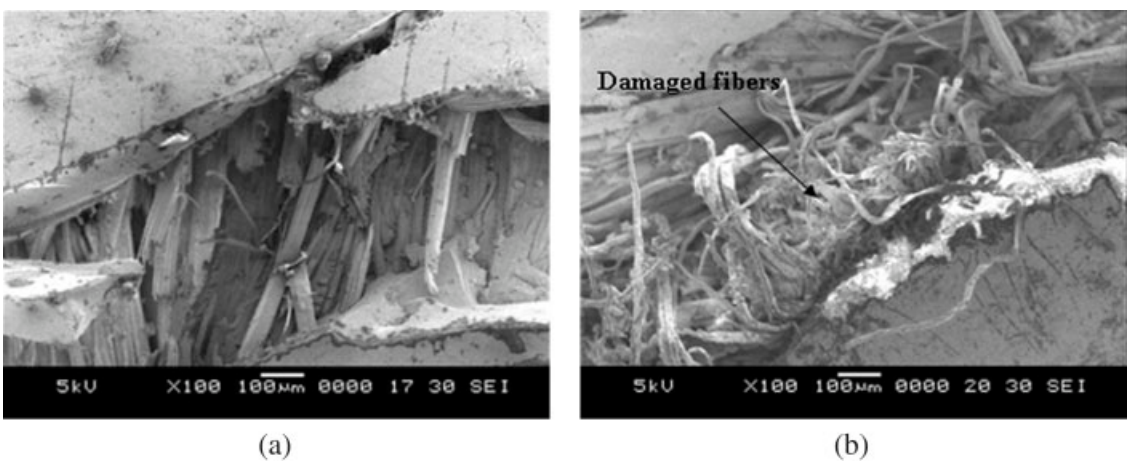

Figure 17 (a) SEM image of fractured surface under flexural load at ×100 magnification before immersion in water and (b) SEM image of fractured surface under flexural load at ×100 magnification after 65 days of immersion in water.

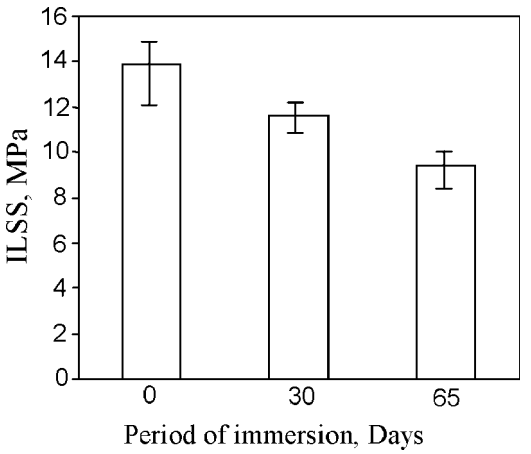

Figure 18 ILSS for different periods of immersion in water.

facilities. We are grateful to Dr Shama Rao, Group Director, Aeronautical Development Agency, Bangalore, Dr. A. C. B. Naidu, Principal, BMS Institute of Technology, Bangalore, for their guidance and encouragement during this work.

References

1. Rout, J.; Mishra, M.; Tripathi S. S.; Nayak, S. K.; Mohanty, A. K. Compos Sci Technol 2001, 61, 1303.
2. Karnani, R.; Krishnan, M.; Narayan, R. Polym Eng Sci 1997, 37, 476.
3. Joshi, S. V.; Drzal, L. T.; Mohanty, A. K.; Arora, S. Compos A 2004, 35, 371.
4. Rao, R. M. V. G. K.; Balasubramanian, N.; Manas, C. J Appl Polym Sci 1981, 26, 4069.
5. Shan, A. N.; Lakkad, S. C. Fiber Sci Technol 1981, 15, 41.
6. Bisanda, E. T. N.; Ansell, M. P. Compos Sci Technol 1991, 41, 165.
7. Seema, J.; Jindal, U. C.; Rakesh, K. J Mater Sci Lett 1993, 12, 558.
8. Karmaker, A. C.; Hoffmann, A.; Hinrichsen, G. J Appl Polym Sci 1994, 54, 1803.
9. Jayamol, G.; Bhagawan, S. S.; Prabhakaran, N.; Sabu, T. J Appl Polym Sci 1995, 57, 843.
10. Kuruvilla, J.; Sabu, T. Polymer 1996, 37, 5139.
11. Jochen, G.; Bledzki, A. K. Compos Sci Technol 1999, 59, 1303.
12. Munikenche Gowda, T.; Naidu, A. C. B.; Chhaya, R. Compos A 1999, 30, 277.
13. Mohanty, A. K.; Khan, A. M.; Hinrichsen, G. Compos Sci Technol 2000, 60, 1115.
14. Singh, B.; Gupta, M.; Anchal, V. Compos Sci Technol 2000, 60, 582.
15. Razera, I. A. T.; Frollini, E. J Appl Polym Sci 2004, 91, 1077.
16. Paul, W.; Jan, I.; Ignaas, V. Compos Sci Technol 2003, 63, 1259.
17. Mallick, P. K. Fiber Reinforced Composites—Materials, Manufacturing and Design, 2nd ed.; Marcel Dekker: New York, 1993; Chapter 4.
18. Gay, D.; Hoa, S. V.; Tsai, S. V. Composite Materials—Design and Applications; CRC Press: Paris, 2003.
19. Bonnian, P.; Bansell, A.R. J Compos Mater 1981, 15, 272.
20. Collingsm, T. A.; Copley, S. M. Composites 1983, 14, 180.
21. Shen, C. H.; Springer, G. S. J Compos Mater 1976, 10, 2.
22. Clark, R. A.; Ansell, M. P. J Mater Sci 1986, 21, 269.
23. Ghasemi Nejhad, M. N.; Parvizi Majidi, A. Composites 1991, 21, 155.
24. Helfilnstine, J. D. Composite Materials: Testing and Design (Fourth Conference), ASTM STP 617, 1977; p 375.
25. Moe Moe, T.; Kin, L. Compos Sci Technol 2003, 63, 375.